

Self-Association of Isoguanine Nucleobases and Molecular Recognition of Alkaline Ions: Tetrad vs Pentad Structures

Michael Meyer^{*,†} and Jürgen Sühnel[‡]

Revotar Biopharmaceuticals AG, Neuendorfstrasse 24a, D-16761 Hennigsdorf, Germany, and Institut für Molekulare Biotechnologie, Beutenbergstrasse 11, D-07745 Jena, Germany

Received: September 6, 2002; In Final Form: November 22, 2002

The formation of both isoguanine tetrad and isoguanine pentad alkali metal ion complexes has been reported in experimental studies. We have performed B3LYP hybrid density functional calculations on complexes between alkali metal ions and cyclic isoguanine tetrads and pentads to study a possible preference of specific ions for either pentads or tetrads. All tetrad cation complexes are strongly nonplanar, except for Li⁺ complexes. Pentads form planar complexes with K⁺ and Rb⁺. For all investigated model systems, the polyad alkali ion interaction is the dominant contribution to the interaction energy. In tetrads, the hydrogen bond pattern changes when passing from the tetrad to the metal–ion-containing complexes. In general, the interaction energy between polyads and alkali metal ions decreases with the size of the ion. For Li⁺, the interaction with the tetrad is stronger, whereas for ions with larger radii the pentad alkali metal ion interaction energy exceeds the corresponding energy for tetrads. A comparison of the interaction energies per base also indicates that the formation of tetrad ion complexes is generally favored for smaller ions, whereas for large ions the difference of the interaction energy per base in tetrads and pentads vanishes. To estimate the performance of the density functional approach for hydrogen-bonded systems, dimers of 6-amino-1H-pyrimidin-2-one, a substructure of isoguanine, have been studied by B3LYP and Møller–Plesset perturbation theory.

Introduction

Molecular recognition of cations is an important feature of several bioorganic ligands. Well-known examples comprise the formation of complexes between alkali ions and ionophoric antibiotics for ion transport through membranes or the selective sequestering of ferric ions by siderophores for iron supply of bacteria.^{1,2} Synthetic siderophores have been developed for specific ion recognition and drug delivery. For an efficient and directed application, these siderophores must be able to recognize cations in a very specific way.

Similarly, metal ions are recognized by nucleic acids and often play a crucial role in structure and function. Guanine (G)-rich sequences are known to adopt unusual tetraplex structures in the presence of metal ions by self-association. From experimental and theoretical studies, it is known that depending on the ion size, the metal ion binding sites are either directly located in the base tetrad centers or between two tetrad planes.^{3,4} Theoretical studies have also shown that the interaction energy between the metal ions and the base tetrads is the dominant contribution to the total interaction energy.⁵ G tetraplexes have a high preference for the alkali ion K⁺, the cation with the highest concentration in cells. Recently, the K⁺-induced and concentration-dependent association of oligonucleotide drug candidates has been used to generate structural changes of G tetraplex structures inside and outside cells required for drug delivery.⁶

Supramolecular chemistry has also taken advantage of the association and recognition principles developed by bioorganic

ligands. For example, the recognition of cations not occurring in biological systems by G tetrads has been investigated and lipophilic guanosine analogues have been used to show the potential of nanostructure formation.^{7,8} In the presence of metal ions, the self-assembly of tetrad building blocks leads to surprisingly regular polymeric columnar aggregates.

Recently, several experimental studies on the self-assembly of isoguanine (iG) nucleobases have been reported. Seela and co-workers have studied the self-aggregation of d(T₄iG₄T₄).⁹ On the basis of ion exchange, high-performance liquid chromatography (HPLC), and circular dichroism (CD)–spectroscopic experiments, they have claimed that in the presence of Na⁺ ions the iG tetraplex is more stable than the corresponding G tetraplex. More recently, this study has been supplemented by an investigation of the self-assembly of oligonucleotides containing iG derivatives. In the presence of Cs⁺, the formation of a pentaplex was observed, whereas tetraplexes were formed with Na⁺ and Rb⁺.¹⁰ Chaput and Switzer have also investigated the cation-assisted self-assembly of oligonucleotides containing iG with K⁺ and Cs⁺ using electrophoretic assays for monitoring strand association.¹¹ In addition to tetraplexes, they also found evidence for the formation of pentaplexes. These authors have proposed a geometric model predicting that the maximum number of nucleobases in a cyclic and (approximately) planar polyad is four for G and five for iG. They have also carried out ab initio calculations on K⁺ and Cs⁺ pentad complexes at the Hartree–Fock level with a small basis set. A direct proof of pentaplex formation of isoguanine derivatives with Cs⁺ has been provided by means of X-ray crystallography.¹² In contrast to the experimental observations mentioned above, recent NMR studies indicate that iG derivatives also form pentad structures with small alkali metal ions.¹³ It should be noted, however, that monomeric ligands have been used by Cai et al.,¹³ whereas the

* To whom correspondence should be addressed. E-mail: m.meyer@revotar-ag.de.

[†] Revotar Biopharmaceuticals AG.

[‡] Institut für Molekulare Biotechnologie.

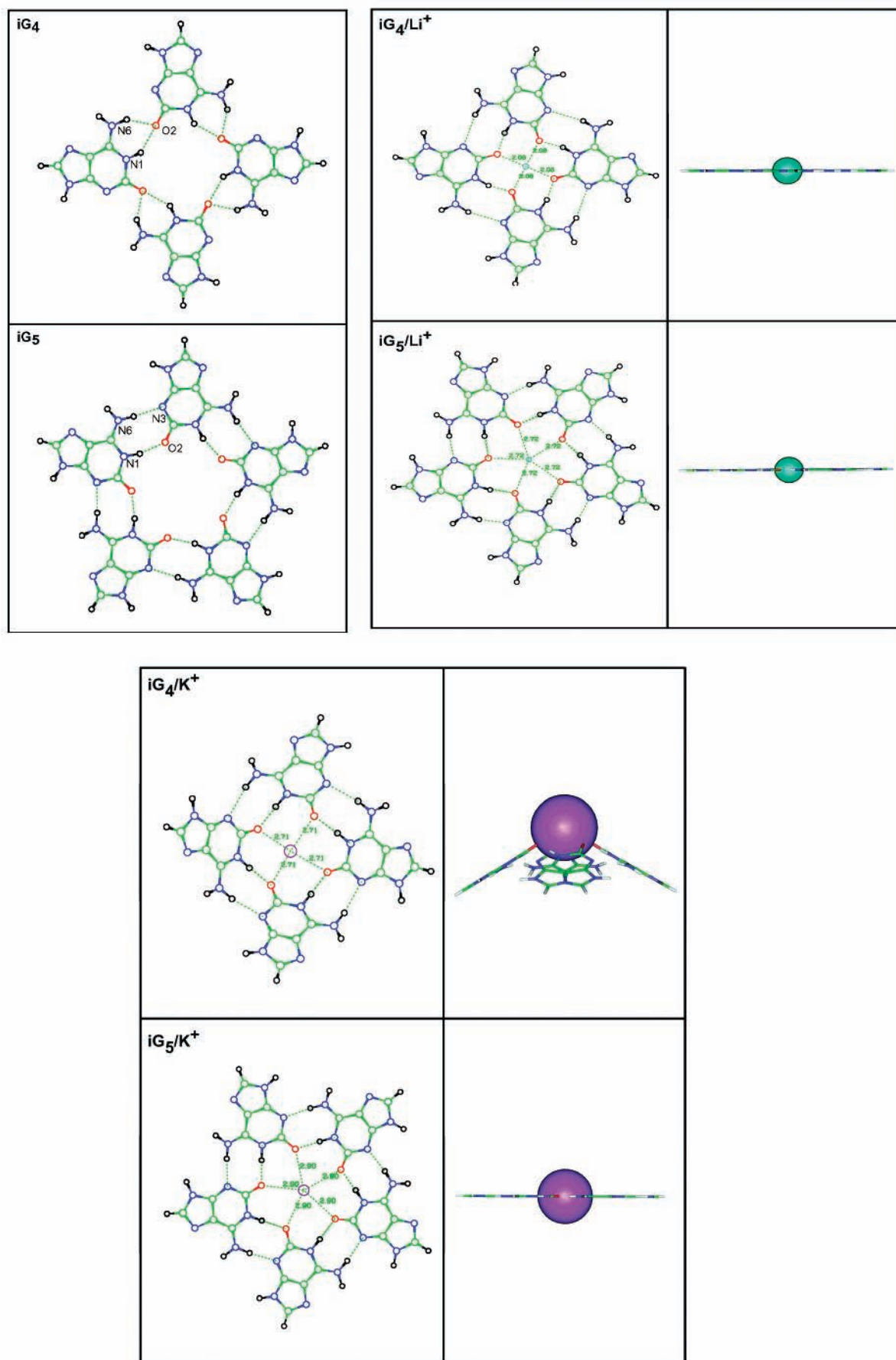


Figure 1. Cyclic isoguanine tetrad and pentad.

assembly of oligonucleotides has been studied in the other cases.^{9–11} Also, other experimental conditions were different.

Quantum chemistry has become a potent tool to analyze the recognition of ions by ligands and to provide models for cation

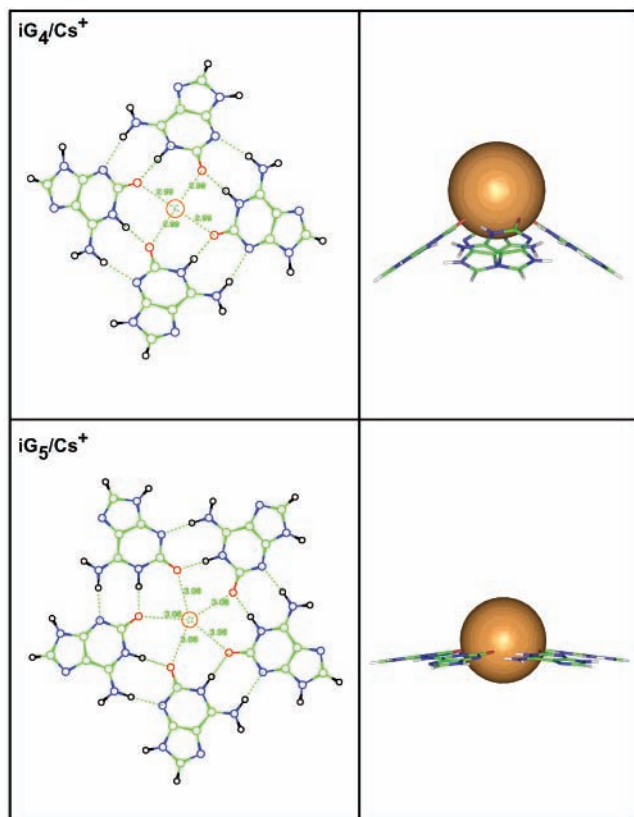


Figure 2. Structure of cyclic isoguanine tetrad and pentad complexes with alkaline ions.

recognition in systems such as siderophores and nucleic acids.^{5,14–22} Ab initio molecular orbital and density functional theory (DFT) studies are very demanding, however, and cannot be applied to complete nucleic acids but are restricted to building blocks such as tetrads. Here, we use the DFT to analyze the recognition of cations by iG, a product of oxidative damage of DNA.

We have used tetrad and pentad/metal ion complexes as structural models to investigate the intermolecular interactions in detail (Figures 1 and 2). These polyad/metal ion complexes are the basic building blocks of the tetraplex and pentaplex structures. The properties of oligonucleotide tetraplex or pentaplex structures may also be affected by nucleic acid stacking, backbone restraints, ion hydration and entropic effects. Nevertheless, the approach adopted can provide information whether the ion dependence of self-association is due to the properties of the metal ion/polyad complexes.

Our calculations are based on DFT with medium-sized basis sets. We present a partition of the energies to compare the base–base interaction in tetrads and pentads and analyze in detail the polyad metal ion interactions for the complete series of alkali cations in order to provide additional guidelines for the design of cation-assisted assemblies of bioorganic ligands. With these calculations, we supplement the geometrical considerations of Chaput and Switzer¹¹ by quantitative interaction energies between the bases and by an additional consideration of the cations in the formation of complexes.

Methods

Initially, the structures of the planar iG tetrads and pentads have been investigated at C_{4h} and C_{5h} symmetry, respectively. Complexes with alkali ions have been generated by placing the

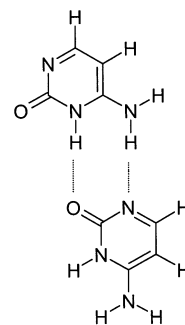


Figure 3. 6-Amino-1H-pyrimidine-2-one dimer.

cations in the central cavity at the origin. Nonplanar C_4 and C_5 symmetric complexes for optimization have been generated by placing the cations on the 4-fold or 5-fold principal axis of symmetry about 2 Å above the polyad plane. Finally, we have also investigated S_4 symmetric tetrad ion complexes. To study nonplanar tetrad and pentad structures without metal ions, we have removed the ions from the optimized metal ion complex structures at C_4 and C_5 symmetry and then performed the optimization of these structures. All calculations have been carried out with the B3LYP hybrid density functional method^{23–25} and the DZVP basis set²⁶ optimized for DFT calculations. For the Cs^+ ion, we have used a relativistic pseudo potential²⁷ in combination with the standard 6-31G(d,p) basis set. Previously, this approach has given a good agreement with all electron calculations for G tetrads and tetrad cation complexes.⁵ Because of the increasing computational effort, we have restricted the B3LYP/DZVP frequency calculations to the tetrad, pentad, and tetrad ion complexes. For the alkali metal ion pentad complexes, stationary points were validated at a lower level (B3LYP/3-21G(d)).

To check the performance of the efficient B3LYP approach, we have also applied Møller–Plesset perturbation theory of second and third order (MP2, MP3) with the 6-31G and 6-311G Gaussian type basis sets supplemented by polarization and diffuse functions to the iG monomer.^{28–31} Furthermore, we performed Hartree–Fock, MP2, and MP3 calculations of the structure and interaction energies for the planar dimer of 6-amino-1H-pyrimidin-2-one to estimate the accuracy of B3LYP/DZVP calculations for hydrogen bond interactions (Figure 3). This complex may be regarded as a substructure of the iG tetrad and pentad. Gaussian98 was used throughout.³²

The polyad interaction energies were calculated according to a previously described scheme using the counterpoise method to correct the basis set superposition error.^{5,33} The most important points are summarized below. The total interaction energy of the tetrads was calculated according to eq 1, where $E(MB_n)$ denotes the energy of the complex formed by the polyad of order 4 or 5 and the alkali ion M. $E(B)$ is the energy of a single base in the full polyad-centered basis.

$$\Delta E = E(MB_n) - nE(B) - E(M) \quad (1)$$

The interaction energy between the polyads and the ion can be estimated with the equation

$$\Delta E^{PM} = E(MB_n) - E(B_n) - E(M) \quad (2)$$

Each base deviates from its ideal monomer geometry when complexes are formed, and the corresponding deformation energy (ΔE^{def}) is the energy difference between the structure

TABLE 1: Total Energies E (H), Energy Differences (kcal/mol) between Isoguanine and Guanine, and Energy Differences between Structures with Planar and Nonplanar Amino Groups at Various Levels of Theory (kcal/mol)

	B3LYP/DZVP	B3LYP/TZVP	MP2/6-31G(d,p)	MP2/6-311G(d,p)
$E(iG)$	-542.62392	-542.71706	-541.02915	-541.22833
$E(iG) - E(G)$	4.64	4.22	7.52	7.78
$\Delta E^{\text{amino}}(iG)$	0.34	0.08	0.41	0.78
$\Delta E^{\text{amino}}(G)$	1.02	0.53	1.47	1.79
	MP2/6-311G(2d,p)	MP2/6-311G(3d,p)	MP2/6-311+G(3dp)	MP3/6-311G(d,p)//MP2/6-311G(d,p)
$E(iG)$	-541.34203	-541.37686	-541.39666	-541.22708
$E(iG) - E(G)$	6.70	7.42	6.83	7.79
$\Delta E^{\text{amino}}(iG)$	0.45	0.49	0.43	0.57
$\Delta E^{\text{amino}}(G)$	1.28	1.62	1.37	1.61

adopted by a single base in the complex and the optimized monomer structure.

$$\Delta E^{\text{T}} = \Delta E + n\Delta E^{\text{def}} \quad (3)$$

Furthermore, the zero point vibration energy difference (ΔZPE) between the polyad and the individual bases contributes to ΔE_0 defined as

$$\Delta E_0 = \Delta E^{\text{T}} + \Delta ZPE \quad (4)$$

For the polyads without ions, eq 1 simplifies to

$$\Delta E = E(B_n) - nE(B) \quad (5)$$

This interaction energy may also be expressed as a sum of pair interaction energies and an adjusted nonadditive term ΔE^{c} . For the pentad, we may write

$$\Delta E = \sum \Delta E^{12} + \sum \Delta E^{13} + \sum \Delta E^{14} + \Delta E^{\text{c}} \quad (6)$$

In this equation, ΔE^{12} denotes the interaction energy between hydrogen-bonded neighbor bases. ΔE^{13} and ΔE^{14} are interactions between nonneighbor polyad bases defined in a cyclic manner. The latter term is absent in tetrads.

Results

iG Monomers. The energy differences of iG and G structures with planar and nonplanar amino groups are summarized in Table 1. Generally, the structures with pyramidal nitrogen atoms are more stable than the planar structures for both nucleobases. For iG, the energy difference between the planar and the nonplanar structures is about 0.5 kcal/mol, whereas the corresponding energy difference is about 1 kcal/mol higher for G. Thus, the tendency to form planar amino groups in polyads is expected to be higher for iG as compared to G. It should be noted that the energy difference is quite stable for iG. On the other hand, for G, this quantity converges only slowly with an increasing basis set as pointed out previously by Šponer et al.³⁴ A higher order perturbation treatment does not show a significant influence on the energy difference.

Therefore, the energy difference between the iG and the G isomers also shows a slow convergence with the basis set. The energy difference between both isomers is about 4.6 kcal/mol at the B3LYP/DZVP level, whereas Møller–Plesset perturbation theory predicts that G is between 5.9 and 7.8 kcal/mol more stable than G at MP2/6-311+G(3d,p) and MP3/6-311G(d,p)//MP2/6-311G(d,p) levels. In summary, we conclude that the B3LYP/DZVP energy difference between planar and nonplanar structures is in reasonable agreement with MP2 calculations employing large basis sets.

TABLE 2: Interaction Energies (ΔE , kcal/mol) and Hydrogen Bond Distances (\AA) of the 6-Amino-1H-pyrimidin-2-one Dimer

method	ΔE	$r(\text{H1}\cdots\text{O2})$	$r(\text{H6}\cdots\text{N3})$
B3LYP/DZVP	-14.04	1.986	2.154
HF/6-31G(d)			
MP2/6-31G(d)	-13.44	1.956	2.081
MP3/6-31G(d)//MP2/6-31G(d)	-13.51		
MP2/6-311G(d,p)//MP2/6-31G(d)	-12.56		
MP2/6-311+G(d,p)//MP2/6-31G(d)	-14.36		
MP2/6-311+G(2d,p)//MP2/6-631G(d)	-14.88		

6-Amino-1H-pyrimidin-2-one Dimer. The interaction energy of the 6-amino-1H-pyrimidin-2-one dimer is -14.04 at the B3LYP/DZVP level (Table 2). This interaction energy is in close agreement with the corresponding data obtained from MP2 single point calculations and large basis sets. The hydrogen bond lengths determined with the DFT method are somewhat larger than the ones determined with the MP2/6-31G(d) method. Hartree–Fock calculations, in contrast, failed to reproduce this hydrogen-bonded dimer structure. MP3 interaction energies obtained with medium-sized basis sets are hardly different from the results predicted by MP2. Because the B3LYP performed reasonably well for the hydrogen-bonded 6-amino-1H-pyrimidin-2-one dimer, we expect that the B3LYP density functional approach is also appropriate for the investigation of hydrogen-bonded iG polyads.

iG Tetrad and Pentad Structures. The planar structures of the iG tetrad and pentad at C_{4h} and C_{5h} symmetry, respectively, correspond to both local energy minima. The H-bond pattern is significantly different in the tetrad and pentad structures (Figure 1, Table 3). Both structures have a N1–H1 \cdots O2 H-bond, that is, however, significantly longer in the tetrad (1.990 \AA) than in the pentad (1.795 \AA). In the tetrad, there is a second H-bond between N6–H6 and the acceptor atom O2 already involved in the N1–H1 \cdots O2 H-bond thereby forming a bifurcated H-bond pattern. On the other hand, in the pentad, the second H-bond occurs between N6–H6 and N3. Again, the tetrad H-bond N6–H6 \cdots O2 is with 1.901 \AA substantially longer than the related pentad H-bond N6–H6 \cdots N3 (1.795 \AA). The tetrad N6–H6 \cdots N3 distance is with 2.645 \AA slightly larger than the usual H-bond distance criterion of 2.5 \AA .

We have also investigated nonplanar structures of iG polyads. A C_5 symmetric start structure derived from the optimized C_s^+ complex by removing the metal ion (see below) converged to the planar C_{5h} symmetric structure. A structure corresponding to S_4 of the tetrad cannot exist for the pentad for symmetry reasons, of course. A nonplanar C_4 symmetric tetrad structure also converged to the planar structure described above. Thus,

TABLE 3: Selected Geometrical Parameters of Polyads and Alkali Metal Ion Isoguanine Polyad Complexes

tetrad	Li ⁺	Na ⁺	K ⁺	Rb ⁺	Cs ⁺
r (M···O2) ^a	2.079	2.322	2.715	2.875	2.990
r (N1–H1···O2)	1.990	1.631	1.686	1.733	1.747
r (N6–H6···N3)	2.645	2.475	2.266	2.123	2.098
r (N6–H6···O2)	1.901				
plane RMS ^b	0.0	0.0	0.724	0.927	0.968
r (M···plane) ^c	0.0	1.769	2.942	3.273	3.596
pentad	Li ⁺	Na ⁺	K ⁺	Rb ⁺	Cs ⁺
r (M···O2)	2.723	2.768	2.900	2.977	3.059
r (N1–H1···O2)	1.795	1.689	1.699	1.735	1.759
r (N6–H6···N3)	1.966	1.882	1.891	1.921	1.941
plane RMS	0.0	0.0	0.0	0.0	0.243
r (M···plane)	0.0	0.0	0.0	0.0	1.152

^a Distance (Å). ^b RMS deviation of polyad atoms from a least squares plane. ^c Height of the metal ion above the RMS polyad plane.

the most stable hydrogen-bonded iG tetrad and pentad structures are planar. This result should be compared to other cyclic tetrad structures formed from one nucleobase only that have planar (C), slightly nonplanar (G,U), or strongly nonplanar (A,T) geometries.^{5,17,35–37}

Tetrad and Pentad Complexes with Alkali Metal Ions. Pentads adopt planar structures of C_{5h} symmetry with K⁺ and Rb⁺ located at the center of the cavity; the Cs⁺ complex, which has a C_5 symmetric structure, is 0.38 kcal/mol more stable than the planar structure. In this case, the cation is located about 1.152 Å above the root mean square (RMS) plane of the pentad as indicated by the height of the cation about the RMS plane of the polyad atoms (Table 3). Planar Li⁺ and Na⁺ complexes do not correspond to a local energy minimum. In contrast, all tetrad complexes except for the Li⁺ complex adopt nonplanar C_4 symmetric structures. As the cation may be located above or below the polyads, there are two equivalent nonplanar structures. The planar C_{4h} symmetric structures of the Na⁺ complex correspond to a transition state between these nonplanar structures as indicated by a single imaginary vibrational frequency of 13 cm⁻¹. For the other complexes, the number of imaginary frequencies increases up to five, the highest frequency being found for Cs⁺ (58 cm⁻¹). Similarly, the energy differences between the planar and the nonplanar structures $E(C_4) - E(C_{4h})$ increase rapidly with the size of the alkali ion. The height of the cations above the RMS polyad plane ranges from 1.769 Å for Na⁺ to 3.596 Å for Cs⁺. The data in Table 3 indicates that in general, the tetrad structures are much more nonplanar than the pentad structure in the Cs⁺ complex since the RMS deviation of the polyad atoms from the least squares plane is much larger. The nonplanar C_4 symmetric structures are less stable than C_{4h} symmetric ones; the S_4 symmetric structures converge to a planar geometry.

In the pentads, a shortening of both H-bonds between neighbor bases is observed when cations are located in the central cavity. This effect is most prominent for Li⁺ and decreases with increasing cation size. The distance between the O2 and the cation increases, of course, from Li⁺ to Cs⁺. Small deviations from the trend from Rb⁺ to Cs⁺ may be attributed to the different techniques applied.

In the metal ion tetrad complexes, no bifurcated H-bonds do exist. Thus, the cations induce a change in the H-bond pattern. This is not surprising, since the cation base interaction is usually much stronger than base–base interactions. In contrast to the polyads without alkali metal ions, the tetrad base–base hydrogen bonds are shorter than the corresponding ones in the pentad. In

TABLE 4: Total Energy (E , H) of Isoguanine Polyads and Interaction Energies (ΔE , kcal/mol)^a

symmetry	iG tetrad C_{4h}	iG pentad C_{5h}
E	-2170.62158	-2713.28017
ΔE	-85.81	-106.25
ΔE^{12}	-16.12	-14.52
ΔE^{13}	-3.05	-1.56
ΔE^{14}		-1.57
ΔE^c	-15.23	-18.00
ΔE^{def}	2.87	2.49
ΔE^T	-74.33	-93.8
$\Delta E^T/n$	-18.58	-18.76
ΔZPE	4.35	5.62
ΔE_0	-69.98	-88.12
$\Delta E_0/n$	-17.50	-17.62

^a The interaction energies are defined in eqs 1–6.

addition, shorter distances between the metal ion and the O2 may be achieved in the tetrad.

Interaction Energies. The interaction energies (ΔE_0) of the tetrad and pentad structures without metal ions amount to -69.98 and -88.12 kcal/mol, respectively (Table 4). The main contributions are the interaction energies between the hydrogen-bonded neighbor bases ΔE .¹² As the hydrogen bond patterns of the tetrads and pentads differ, it is not surprising that these interaction energies are different (tetrad, -16.12 kcal/mol; pentad, -14.52 kcal/mol). The stronger interaction in the tetrad also induces a higher deformation energy (ΔE^{def}) of the individual bases in the tetrad. Zero point energy contributions (ΔZPE) to the interaction energy are smaller than the sum of the deformation energies in each polyad. The interaction energy increases with the number of bases, but when the interaction energies are normalized by the number of bases n ($\Delta E^T/n$ or $\Delta E_0/n$), it turns out that there is almost no difference between the tetrad and the pentad. At first sight, this is surprising in view of the fact that ΔE^{12} is more negative for tetrads than for pentads. However, this effect is counterbalanced, at least in part, by the more negative cooperativity contribution in the pentad.

The interaction energies of the cation polyad complexes exceed the interaction energies of the metal free polyads dramatically since the interaction between the bases and the cation becomes the most important energy contribution (Tables 4 and 5). The interaction energies between the polyads and the alkali metal ion (ΔE^{PM}) show clear trends. Their absolute values decrease from Li⁺ to Cs⁺ for both polyad types. The interaction energy between the tetrad and the alkali metal ion decreases from -143.01 kcal/mol for Li⁺ to -72.05 kcal/mol for Cs⁺, whereas the corresponding interaction energy for the pentad complexes decreases from -120.02 kcal/mol for Li⁺ to -83.33 kcal/mol for Cs⁺. This means that the interaction energy between the tetrad and the small cation Li⁺ is stronger than the one between the pentad and the Li⁺. For ions with large radii, the opposite relation holds. For Na⁺, the interaction energies are of similar magnitude.

In the C_{5h} structure of the Cs⁺ pentad complex, a weaker interaction energy of -82.35 kcal/mol between the pentad and the cation is found than in the planar complex. This means that Cs⁺ does not fit in an optimal way into the central cavity.

Discussion

The stability of base polyad metal ion complexes is primarily governed by base–base H-bond and by metal ion base interactions. The optimized iG tetrad and pentad structures are both planar but exhibit a different base–base hydrogen bond pattern: two bifurcated hydrogen bonds between the donor groups

TABLE 5: Total Energies (H), Interaction Energies (ΔE), and Deformation Energies (ΔE^{def}) of Alkali Metal Ion Tetrad and Pentad Complexes (kcal/mol) Calculated at the B3LYP/DZVP Level^a

tetrad	Li ⁺	Na ⁺	K ⁺	Rb ⁺	Cs ⁺
symmetry	C_{4h}	C_4	C_4	C_4	C_4
E	-2178.09312	-2332.84608	-2770.42448	-5110.33037	-2190.43659
$E(C_4) - E(C_{4h})$	0.02	-1.39	-10.67	-16.30	-27.40
ΔE	-206.63	-185.62	-159.67	-151.41	-153.45
ΔE^{PM}	-143.01	-113.53	-83.25	-74.53	-72.05
ΔE^{def}	4.48	4.10	3.72	3.56	4.25
ΔE^{T}	-188.71	-169.22	-144.79	-137.17	-136.45
$\Delta E^{\text{T}}/n$	-47.18	-42.31	-36.20	-34.29	-34.11
$\Delta E^{\text{PM}}/E^{\text{T}}$	0.76	0.67	0.57	0.54	0.53
ΔZPE	6.17	6.21	6.09	5.87	6.02
ΔE_0	-182.54	-163.01	-138.70	-131.30	-130.43
N_{im}^b	0	0	0	0	0
pentad	Li ⁺	Na ⁺	K ⁺	Rb ⁺	Cs ⁺
symmetry	C_{5h}	C_{5h}	C_{5h}	C_{5h}	C_5
E	-2720.72445	-2875.50495	-3313.10780	-5653.016626	-2733.04906
$E(C_5) - E(C_{5h})$					0.38
ΔE	-213.22	-209.81	-198.73	-192.05	-192.37
ΔE^{PM}	-120.02	-114.34	-98.29	-89.59	-83.33
ΔE^{def}	4.34	4.19	3.82	3.67	4.06
ΔE^{T}	-191.52	-188.86	-179.63	-173.70	-172.07
$\Delta E^{\text{T}}/n$	-38.30	-37.77	-35.93	-34.74	-34.41
$\Delta E^{\text{PM}}/E^{\text{T}}$	0.63	0.61	0.55	0.52	0.48
N_{im}^b	4	2	0	0	

^a The interaction energies are defined in eqs 1–6. ^b Number of imaginary vibrational frequencies; B3LYP/3-21G(d) has been used for the pentad complexes.

N6–H6 and N1–H1 and the acceptor atom O2 in the tetrad and two separate H-bonds N6–H6···N3 and N1–H1···O2 in the pentad. In the metal ion polyad complexes, all structures adopt a uniform pattern with two separate H-bonds. Planar tetrads and Li⁺ tetrad complexes correspond to local energy minima. Planar pentads with a larger central cavity correspond to local energy minima in the absence of alkali metal ions and in the presence of K⁺ and Rb⁺. Li⁺ and Na⁺ appear to be too small for the coordination by all pentad O2 atoms, whereas Cs⁺ is too large to fit optimally into the central cavity. The location of this cation above the pentad plane agrees in a qualitative sense with the geometry found in the X-ray structure¹³ and with the computational results obtained by Chaput and Switzer.¹¹

It should be noticed that all hydrogen bonds in the pentad and pentad ion complexes are significantly shorter than in the 6-amino-1H-pyrimidin-2-one dimer. In the tetrad, the H1···O2 hydrogen bond is always shorter in the complexes with cations. The hydrogen bond between the amino group and N3 is long in complexes with small cations and short in complexes with ions of large radii.

The distances between the base–base H-bond donor and acceptor atoms N6···N3 (2.94 Å) and N1···O2 (2.78 Å) in the C_5 symmetric Cs⁺iG₅ complex are in reasonable agreement with the average distances observed in the crystal structure (2.82 and 2.73 Å).¹² The height of the Cs⁺ ion above the pentad plane of 1.15 Å, however, is significantly smaller than half of the distance between two pentads in the crystal structure (3.3 Å). It is to be expected that an extended model system with the Cs⁺ ion sandwiched between two pentads will lead to a better agreement with the X-ray structure. The importance of the environment has been pointed out recently for the AT pair by Guerra and co-workers.³⁹

All of the metal ion tetrad complexes except for Li⁺ are nonplanar and exhibit for K⁺, Rb⁺, and Cs⁺ rather large heights of the metal ions above the RMS tetrad plane (Table 3). These large distances may prevent these building blocks from being optimally inserted into a nucleic acid environment.

The pair interaction energies ΔE^{12} in the tetrad and pentad exceed the interaction energy of 6-amino-1H-pyrimidin-2-one dimer. In the absence of metal ions, the iG tetrad interaction energy (ΔE_0) of -69.98 kcal/mol is more negative than the corresponding interaction energy of the G tetrad (-61.28 kcal/mol). Taking into account further cyclic tetrads, the order of the absolute values of interaction energies (ΔE_0) is iG > GCGC > G > C > U > T.¹⁷

The order of ΔE_0 is changed to G > GCGC > C > U > T when complexes with alkaline ions are formed.³⁸ The total interaction energy of iG tetrad complexes with Li⁺ and Na⁺ exceeds even the ones of the corresponding G tetrad complexes. Data for Rb⁺ and Cs⁺ are not available for the G tetrads. It is in agreement with the experimental observation that certain iG tetraplex structures are more stable than the corresponding G tetraplexes.⁹ Like in other tetrad ion complexes, the interaction energy is dominated by the contribution of the polyad cation interaction energy (ΔE^{PM}).

To address the interaction between alkali metal ions and polyads in more detail, we have calculated the interaction energy between the cation and the polyad (ΔE^{PM} ; Table 5). This quantity decreases with cation size for both tetrads and pentads, but for Li⁺, the interaction with the tetrad is stronger than with the pentad, whereas the larger alkali metal ions have more negative interaction energies for the pentad complexes. Furthermore, we have calculated the normalized interaction energy per base ($\Delta E^{\text{T}}/n$) (Tables 4 and 5). For the metal free tetrad and pentad structures, this quantity differs by only 0.18 kcal/mol (Table 4). When passing to polyad/metal ion complexes, there are significant differences in $\Delta E^{\text{T}}/n$ between tetrads and pentads for the small ions Li⁺ (tetrad, -47.18 kcal/mol; pentad, -38.80 kcal/mol) and Na⁺ (tetrad, -42.31 kcal/mol; pentad, -37.77 kcal/mol). When the ordinary number and thus the size of the alkali ions increases, this energy difference vanishes and the pentads are even slightly favored for Rb⁺ and Cs⁺. Therefore, the observed equilibrium between tetrads and pentads may be shifted toward the pentad complexes. Because we are

studying the interaction of cations with a single polyad, our model system considers only a part of the experimental systems with stacked polyads. Therefore, it is clear that we cannot fully describe the recognition properties of tetraplexes and pentaplexes. However, our calculations indicate that even a single polyad has the ability to bind cations in a size-dependent manner. In fact, for G tetrads, a recognition of small cations within the tetrad plane and of large ions between two tetrad planes has been observed. For a quantitative explanation of ion selectivity, the additional consideration of the interaction between alkali metal ions and two stacked tetrads and also of solvation and entropic effects is clearly necessary. However, this is beyond the scope of our study.

B3LYP calculations are suitable for the study of hydrogen-bonded nucleobases since there is a good agreement between B3LYP and MP2 and MP3 calculations for the structure and interaction energies for 6-amino-1H-pyrimidin-2-one dimer. This corresponds to several other studies using the DFT and MP2 method.^{40–42} Single point MP3 calculations provide interaction energies that are not much different from MP2 calculations.

To sum up, we have shown that density functional calculations are a helpful tool to analyze the structures and energies of alkali ion polyad complexes. We have shown that cations are capable of changing the hydrogen bond pattern of tetrads, and furthermore, we have supplemented geometrical requirements for the bases for a possible self-assembly to polyads with energetical considerations. Our calculations indicate that the interaction energy per base is most favorable for tetrad complexes with small cations whereas large ions may induce a pentad formation. Our results supplement the qualitative working design used by Chaput and Switzer¹¹ by a more quantitative treatment. An application of this type of analysis to other polyad cation systems may provide rules for the design of specific ligands.

Acknowledgment. We thank C. Switzer (University of California, Riverside) for providing us with his pentad coordinates.

References and Notes

- (1) Roosenberg, J. M.; Lin, Y.-M.; Lu, Y.; Miller, M. J. *Curr. Med. Chem.* **2000**, *7*, 159–197.
- (2) Riddell, F. G. *Chirality* **2002**, *14*, 121–125.
- (3) Parkinson, G. N.; Lee, M. P. H.; Neidle, S. *Nature* **2002**, *417*, 876–880.
- (4) Patel, D. J.; Bouaziz, S.; Kettani, A.; Wang, Y. Structures of Guanine-Rich and Cytosine-Rich Quadruplexes Formed In Vitro by Telomeric, Centromeric, and Triplet Repeat Disease DNA Sequences. In *Oxford Handbook of Nucleic Acid Structure*; Neidle, S., Ed.; Oxford University Press: Oxford, 1999; pp 389–453.
- (5) Meyer, M.; Steinke, T.; Brandl, M.; Sühnel, J. *J. Comput. Chem.* **2001**, *22*, 109–124.
- (6) Jing, N.; Xiong, W.; Guan, Y.; Pallansch, L.; Wang, S. *Biochemistry* **2002**, *41*, 5397–5403.
- (7) Kotch, F. W.; Fettingner, J. C.; Davis, J. T. *Org. Lett.* **2000**, *2*, 3277–3280.
- (8) Mezzina, E.; Mariani, P.; Itri, R.; Masiaero, S.; Pieraccini, S.; Spada, G. P.; Spinozzi, F.; Davis, J. T.; Gottarelli, G. *Chem. Eur. J.* **2001**, *7*, 388–395.
- (9) Seela, F.; Wei, C.; Melenewki, A. *Nucleic Acids Res.* **1996**, *24*, 4940–4945.
- (10) Seela, F.; Kroschel, R. *Bioconjugate Chem.* **2001**, *12*, 1043–1050.
- (11) Chaput, J. C.; Switzer, C. *Proc. Natl. Acad. Sci. U.S.A.* **1999**, *96*, 10614–10619.
- (12) Cai, M.; Marlow, A. L.; Fettingner, J. C.; Fabris, D.; Haverlock, T. J.; Moyer, B. A.; Davis, J. T. *Angew. Chem.* **2000**, *112*, 1339.
- (13) Cai, M.; Sidorov, V.; Lam, Y.-F.; Flowers, R. A.; Davis, J. T. *Org. Lett.* **2000**, *2*, 1665–1668.
- (14) Hay, B. P.; Dixon, D. A.; Vargas, R.; Garza, J.; Raymond, K. N. *Inorg. Chem.* **2001**, *40*, 3922–3935.
- (15) Meyer, M.; Trowitzsch-Kienast, W. *Theochem* **1997**, *418*, 93–98.
- (16) Meyer, M.; Schnurre, R.; Reissbrodt, R.; Trowitzsch-Kienast, W. *Z. Naturforsch. C* **2001**, *56*, 540–546.
- (17) Meyer, M.; Schneider, C.; Brandl, M.; Sühnel, J. *J. Phys. Chem. A* **2001**, *105*, 11560–11573.
- (18) Gu, J.; Leszczynski, J. *J. Phys. Chem. A* **2002**, *106*, 529–532.
- (19) Gu, J.; Leszczynski, J. *J. Phys. Chem. A* **2001**, *105*, 10366–10371.
- (20) Russo, N.; Toscano, M.; Grand, A. *J. Am. Chem. Soc.* **2001**, *123*, 10272–10279.
- (21) Burda, J. V.; Šponer, J.; Leszczynski, J. *Phys. Chem. Chem. Phys.* **2001**, *3*, 4404–4411.
- (22) Hobza, P.; Leszczynski, J.; Šponer, J. *Theochem* **2001**, *573*, 43–53.
- (23) Becke, A. D. *J. Chem. Phys.* **1993**, *98*, 5648–5652.
- (24) Lee, C.; Yang, G.; Parr, R. G. *Phys. Rev. B* **1988**, *37*, 785–789.
- (25) Stephens, P. J.; Delvin, F. J.; Chabalowski, C. F.; Frisch, M. J. *J. Phys. Chem.* **1994**, *98*, 11623–11627.
- (26) Godbout, N.; Salahub, D. R.; Andzelm, J.; Wimmer, E. *Can. J. Chem.* **1992**, *70*, 560–571.
- (27) Ross, R. B.; Ermler, W. C.; Christiansen, P. A. *J. Chem. Phys.* **1990**, *93*, 6654.
- (28) Ditchfield, R.; Hehre, W. J.; Pople, J. A. *J. Chem. Phys.* **1971**, *54*, 724.
- (29) Krishnan, R.; Binkley, J. S.; Seeger, R.; Pople, J. A. *J. Chem. Phys.* **1980**, *72*, 650.
- (30) Frisch, M. J.; Pople, J. A.; Binkley, J. S. *J. Chem. Phys.* **1984**, *80*, 3265.
- (31) Clark, T.; Chandrasekhar, J.; Spitznagel, G. W.; Schleyer, P. v. R. *J. Comput. Chem.* **1983**, *4*, 294.
- (32) Frisch, M. J.; Trucks, G. W.; Schlegel, H. B.; Scuseria, G. E.; Robb, M. A.; Cheeseman, J. R.; Zakrzewski, V. G.; Montgomery, J. A., Jr.; Stratmann, R. E.; Burant, J. C.; Dapprich, S.; Millam, J. M.; Daniels, A. D.; Kudin, K. N.; Strain, M. C.; Farkas, O.; Tomasi, J.; Barone, V.; Cossi, M.; Cammi, R.; Mennucci, B.; Pomelli, C.; Adamo, C.; Clifford, S.; Ochterski, J.; Petersson, G. A.; Ayala, P. Y.; Cui, Q.; Morokuma, K.; Malick, D. K.; Rabuck, A. D.; Raghavachari, K.; Foresman, J. B.; Cioslowski, J.; Ortiz, J. V.; Stefanov, B. B.; Liu, G.; Liashenko, A.; Piskorz, P.; Komaromi, I.; Gomperts, R.; Martin, R. L.; Fox, D. J.; Keith, T.; Al-Laham, M. A.; Peng, C. Y.; Nanayakkara, A.; Gonzalez, C.; Challacombe, M.; Gill, P. M. W.; Johnson, B. G.; Chen, W.; Wong, M. W.; Andres, J. L.; Head-Gordon, M.; Replogle, E. S.; Pople, J. A. *Gaussian 98*; Gaussian, Inc.: Pittsburgh, PA, 1998.
- (33) Boys, S. F.; Bernardi, F. *Mol. Phys.* **1970**, *19*, 553–577.
- (34) Šponer, J.; Leszczynski, J.; Hobza, P. *J. Biomol. Struct. Dyn.* **1996**, *14*, 117–135.
- (35) Meyer, M.; Brandl, M.; Sühnel, J. *J. Phys. Chem. A* **2001**, *105*, 823–825.
- (36) Gu, J.; Leszczynski, J. *Chem. Phys. Lett.* **2001**, *335*, 465–474.
- (37) Gu, J.; Leszczynski, J. *Chem. Phys. Lett.* **2002**, *351*, 403–409.
- (38) Meyer, M.; Sühnel, J. *J. Biomol. Struct. Dyn.* **2003**, *20*, 507–518.
- (39) Guerra, C. F.; Bickelhaupt, F. M.; Snijders, J. G.; Baerends, E. J. *J. Am. Chem. Soc.* **2000**, *122*, 4117–4128.
- (40) Meyer, M.; Sühnel, J. *J. Biomol. Struct. Dyn.* **1997**, *15*, 619–624.
- (41) Brandl, M.; Meyer, M.; Sühnel, J. *J. Biomol. Struct. Dyn.* **2001**, *18*, 545–555.
- (42) Brandl, M.; Meyer, M.; Sühnel, J. *J. Phys. Chem. A* **2001**, *104*, 11177–11187.